Journal of Applied Mechanics and Technical Physics, Vol. 42, No. 2, pp. 358–362, 2001

DISTORTION OF THE WAVE PROFILES IN AN ELASTOPLASTIC BODY UPON SPALLING

G. I. Kanel'

UDC 532.593

The distortion of wave profiles in measuring the spall strength of elastoplastic materials is analyzed. An expression for the velocity of an elastic compression wave that overtakes a plastic rarefaction wave is obtained. It is shown that, depending on the ratio between the stress gradients in the plastic rarefaction wave and the overtaking compression wave, the front velocity of the compressive wave varies in the limits between the velocities of the longitudinal perturbations and the perturbations of volume expansion or compression.

The dynamic tensile strength of materials is studied by recording the spalling phenomena occurring upon reflection of a pulse of one-dimensional shock-wave compression from the free surface of a body under submicrosecond loading [1]. The interference of the incident and reflected waves causes rarefaction inside the body which is responsible for high-rate failure. The magnitude of the spalling-rupture stress (spall strength of the material) is determined by measuring the profile of the free-surface velocity as a function of time $u_{fs}(t)$. As a result of relaxation of the tensile stress in the failure, a compression wave which reaches the surface of the body to form a so-called spalling pulse on the profile $u_{fs}(t)$ is generated.

Analyzing the interaction between the incident and reflected waves by the method of characteristics, one obtains a relation between the stress in the spalling plane σ^* and the difference Δu_{fs} between the maximum velocity of the surface in the compression pulse u_0 and its velocity ahead of the spalling-pulse front u_m. In the linear approximation, this relation has the form [2]

$$\sigma^* = \rho_0 c_0 \Delta u_{fs}/2, \qquad (1)$$

where ρ_0 and c_0 are the density of the material and the velocity of sound in it, respectively. Taking into account the nonlinearity of compressibility introduces an insignificant correction into (1).

For an elastoplastic material, it is necessary to infer which velocity of sound should be used in (1): the velocity of elastic longitudinal perturbations $c_l = \sqrt{[K + (4/3)G]/\rho}$ (K is the bulk modulus and G is the shear modulus) or the velocity of volume expansion or compression $c_b = \sqrt{K/\rho}$ which corresponds to the perturbation velocity in the plastic-deformation region.

Figure 1 shows the longitudinal stress σ_x versus the mass velocity u_p for wave interactions occurring when the compression pulse reflects from the free surface of a body. The dashed curve shows the average pressure p as a function of the mass velocity. The curve H shows the shock adiabat, the curves S_i and S_r show unloading trajectories in the incident and reflected rarefaction waves, respectively, and the curves $R_{\rm pl}$ and $C_{\rm el}$ show the trajectories of state change along the C_+ characteristics in the plastic-tension region before spalling and in the elastic-compression region after spalling, respectively. The initial slope of the shock adiabat is $d\sigma_x/du = \rho c_l$ before reaching the elastic limit σ_g and $d\sigma_x/du = \rho c_b$ in the plastic-deformation region beyond the elastic limit. After shock compression, the rarefaction is elastoplastic as well. If the intensity of the shock

Institute of Thermal Physics of Extremal States, Joint Institute of High Temperatures, Russian Academy of Sciences, Moscow 127412. Translated from Prikladnaya Mekhanika i Tekhnicheskaya Fizika, Vol. 42, No. 2, pp. 194–198, March–April, 2001. Original article submitted May 11, 1999.

 0021-8944/01/4202-0358 $25.00

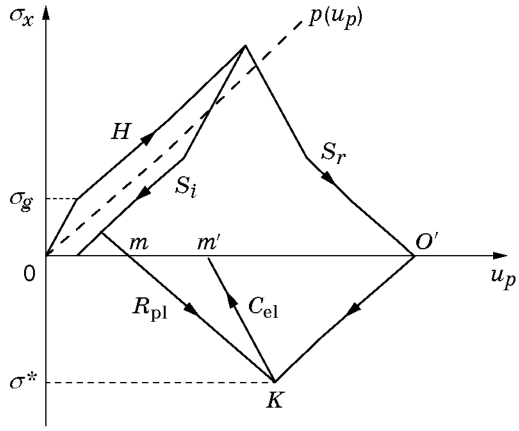

Fig. 1

compression pulse exceeds the quantity $2\sigma_g$, tension is generated in the plastic region owing to interaction between the incident and reflected rarefaction waves.

Novikov, Divnov, and Ivanov [3] note that when the fracture begins, plastic tension in the spalling layer becomes elastic compression. Because of this, the propagation velocity of the spalling-pulse front is equal to the longitudinal velocity of sound c_l, whereas the descending branch of the compression pulse propagates with the volume velocity of sound $c_b < c_l$ in front of it. As a result, the profile of the free-surface velocity is distorted, and the surface-velocity decrement in (1) $\Delta u_{fs} = u_0 - u_{m'}$ is smaller than that in the case where the yield point is ignored ($\Delta u_{fs} = u_0 - u_m$). According to [3], the rupture stress is determined by the point at which the Riemann trajectory $O'K$ with the slope ρc_b corresponding to the tail C_- characteristics of the reflected rarefaction wave intersects the trajectory $m'K$ with the slope $-\rho c_l$ corresponding to the C_+ characteristics of the spalling-pulse front (Fig. 1). The point m' corresponds to the free-surface velocity ahead of the spalling-pulse front. In this approximation, we obtain

$$\sigma_c^* = \rho_0 c_l \Delta u_{fs} (1 + c_l/c_b)^{-1}. \tag{2}$$

In relation (2), the spalling thickness is ignored. At the same time, it is obvious that distortion of the profiles of the free-surface velocity depends on the spalling thickness and the shape of the shock-compression pulse (this is supported by experimental data). Consequently, when used to process experimental data obtained under varied loading conditions, relation (2) can give different values of strength even though its value is constant. To take this fact into account, Romanchenko and Stepanov [4] introduced the correction $\Delta\sigma$ into relation (2):

$$\sigma_c^* = \rho_0 c_l \Delta u_{fs} \frac{1}{1 + c_l/c_b} + \Delta\sigma, \qquad \Delta\sigma = \frac{1}{2} \frac{d\sigma}{dt}\Big|_{C_-} h\Big(\frac{1}{c_b} - \frac{1}{c_l}\Big). \tag{3}$$

Here $d\sigma/dt\Big|_{C_-}$ is the stress gradient along the tail C_- characteristic of the reflected rarefaction wave, which is equal to twice the gradient of the descending branch of the compression pulse, and h is the thickness of the spalling layer. Introduction of the correction $\Delta\sigma$ is substantiated in [4]. It is assumed that introduction of $\Delta\sigma$ allows one to determine the value of u_{fs} that would occur ahead of the spalling-pulse front if the recorded profile of $u_{fs}(t)$ was not distorted because of the difference in the wave velocities. However, in this case, one should use the volume velocity of sound c_b in (3) rather than its combination with c_l. Gluzman and Kanel' [5] proposed a corresponding relation

$$\sigma^* = \rho_0 c_b (\Delta u_{fs} + \delta)/2. \tag{4}$$

According to [5], the correction δ is calculated under the assumption of superposition of the incident rarefaction wave and the spalling pulse with allowance for the free-surface velocity gradients $\dot u_1$ and $\dot u_2$ measured in front of the spalling-pulse front and in the spalling pulse itself, respectively:

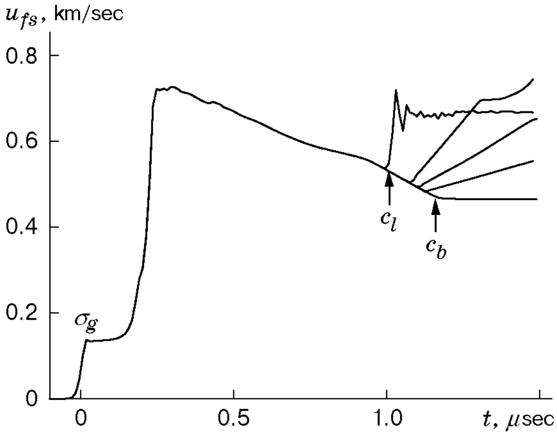

Fig. 2

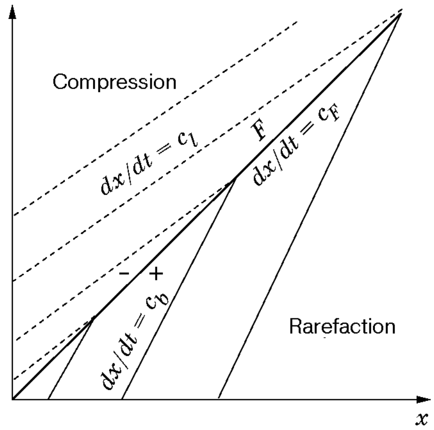

Fig. 3

$$\delta = \Big(\frac{h}{c_b} - \frac{h}{c_l}\Big)\frac{|\dot{u}_1 \dot{u}_2|}{|\dot{u}_1| + \dot{u}_2}. \tag{5}$$

Here the dot denotes differentiation with respect to time.

The fact that, the spall strength can be determined by different methods with the use of same measuring technique shows that the analysis is not sufficiently advanced and calls for more careful study of wave interaction under spalling conditions in an elastoplastic body.

Figure 2 shows results of numerical modeling of the interaction between the overtaking compression and rarefaction waves in an elastoplastic body. On the boundary of the plate, a triangular shock-compression pulse was induced. Initially, the boundary velocity increased linearly and it then increased for 1 μsec, which generated the second compression wave in the plate. In the calculations, the steepness of the second compression wave was varied. The profiles of the free-surface velocity shown in Fig. 2 illustrate the dependence of the velocity of the second-wave front on its steepness. If the second wave is a shock wave, the velocity of its front is equal to the longitudinal velocity of sound. As the steepness of the second wave decreases, the propagation velocity of its front decreases and approaches the volume velocity of sound. Measurements performed under similar conditions [6] show that the velocity of the second compression wave of low intensity lies in the range between c_l and c_b.

To obtain an expression for the velocity of the second-wave front, we consider the x–t (distance–time) diagram shown in Fig. 3. The diagram shows the C_+ characteristics of the initial plastic rarefaction wave followed by the compression wave. The curve F shows the trajectory of the front of the elastic compression wave propagating at the velocity c_F ($c_l \geqslant c_F \geqslant c_b$). With allowance for the angular-momentum equation in the Lagrange coordinates, for the flow on the right of the trajectory F, the rate of change in the stress along the trajectory is given by

$$\frac{d\sigma_x}{dt}\Big|_F = \dot{\sigma}^+ - c_F \rho_0 \dot{u}^+.$$

Similarly, to the left of the trajectory F, we obtain

$$\frac{d\sigma_x}{dt}\Big|_F = \dot{\sigma}^- - c_F \rho_0 \dot{u}^-.$$

In these equations, the plus and minus superscripts denote the parameters on the right and on the left of the trajectory F, respectively.

With allowance for the continuity equation, the mass-velocity gradient on the right of the trajectory has the form

$$\frac{du}{dt}\Big|_F = \dot{u}^+ + c_F \rho_0 \dot{V}^+.$$

Since the deformation ahead of the second wave is assumed to be plastic, we have $\dot{V} = -\dot{\sigma}_x/(\rho_0^2 c_b^2)$. Hence,

$$\left.\frac{du}{dt}\right|_F = \dot{u}^+ - \frac{c_F \dot{\sigma}_x^+}{\rho_0 c_b^2}.$$

On the left of the trajectory F, plastic expansion becomes elastic compression, and, hence, the mass-velocity gradient in this region is given by

$$\left.\frac{du}{dt}\right|_F = \dot{u}^- - \frac{c_F \dot{\sigma}_x^-}{\rho_0 c_l^2}.$$

If there are no discontinuities in the flow, the stress and mass-velocity gradients on either side of the trajectory F must coincide. In this case, we obtain two equations for the velocity of the front of the elastic-compression wave overtaking the plastic rarefaction wave:

$$c_F = \frac{\dot{\sigma}_x^+ - \dot{\sigma}_x^-}{\rho_0(\dot{u}^+ - \dot{u}^-)}, \qquad c_F = \frac{\dot{u}^+ - \dot{u}^-}{\dot{\sigma}_x^+/(\rho_0 c_b^2) - \dot{\sigma}_x^-/(\rho_0 c_l^2)}. \tag{6}$$

Eliminating $\dot{u}^+ - \dot{u}^-$ from (6), we obtain the following relation between the velocity of the second elastic wave and the stress gradients in the second wave and ahead of its front:

$$c_F = c_b c_l \sqrt{\frac{\dot{\sigma}_x^+ - \dot{\sigma}_x^-}{\dot{\sigma}_x^+ c_l^2 - \dot{\sigma}_x^- c_b^2}}. \tag{7}$$

Here $\dot{\sigma}_x^+$ and $\dot{\sigma}_x^-$ are opposite in sign. In accordance with the solution obtained, the front of the overtaking compression wave propagates with the longitudinal velocity of sound only in two limiting cases: 1) the stress gradient vanishes in front of it; 2) the overtaking wave is a shock wave ($\dot{\sigma}_x^- \to \infty$).

As the triangular compression pulse reflects from the free surface of the body, the interference of the incident and reflected rarefaction waves develops in such a manner that in each section of the plate, a constant tensile stress occurs up to the moment at which the spalling pulse arrives, i.e., $\dot{\sigma}_x^+ = 0$. Consequently, according to (7), the spalling-pulse front propagates with the longitudinal velocity of sound $c_F = c_l$ independently of its steepness. In this case, relations (2) and (4) give the same value of the rupture stress provided the correction δ in (4) is calculated as follows:

$$\delta = (h/c_b - h/c_F)|\dot{u}_1|. \tag{8}$$

Here $c_F = c_l$. The spall strength is usually measured by loading plane specimens by impact of a plate, which induces a shock-compression pulse having a plateau of finite duration. In this case, the stresses in the cross sections of the specimen are not constant in front of the spalling-pulse front; therefore, some characteristics of the elastic front of the spalling pulse vanish upon interaction with the plastic rarefaction wave in front of it (Fig. 3). Consequently, relation (2) is not valid in this case, even though the spalling pulse has a shock front. At the moment of spalling, the stress is calculated by relation (4) with allowance for correction (8), where $c_F \neq c_l$ is determined from (7). For an idealized trapezoidal pulse of shock loading, the quantity c_F can be obtained by averaging its values with allowance for the fact that $\dot{\sigma}_x^+ \approx 0$ near the free surface and $\dot{\sigma}_x^+ \approx \rho c_b \dot{u}_1/2$ and $\dot{\sigma}_x^- = \rho c_l \dot{u}_2/2$ in the neighborhood of the spalling plane.

In all the above-mentioned approaches, the quantities σ^* and δ are calculated under the assumption of instantaneous failure concentrated in the spalling plane. In fact, the fracture velocity determined by a number of activated fracture nuclei and their growth rate cannot be arbitrarily large. Since the fracture kinetics is not known *a priori*, the extrapolation of the segments of the profile $u_{fs}(t)$, which is used to estimate the quantity δ, is not substantiated. Therefore, the spall strength should be measured in such a manner that the quantity δ decreases to the minimum value. The minimum distortions $u_{fs}(t)$ occur for a triangular pulse of shock loading. In this case, relation between the measured velocity decrement Δu_{fs} and the correction δ_t in (4) has the form

$$\delta_t = \frac{1}{2}\,\Delta u_{fs}\Big(\sqrt{\frac{3(1-\nu)}{1+\nu}} - 1\Big),$$

where ν is Poisson's ratio. For $\nu = 0.30$–0.35, the value of δ_t is 10–14% of the measured value of Δu_{fs}. Since the steepness of the spalling pulse is not, as a rule, smaller than that of the rarefaction wave in front of it, the correction calculated by (5) is $(0.5$–$1)\delta_t$, i.e., the possible error in determining the spall strength by relations (4) and (5) does not exceed 5–7%, which correlates with the error of experimental data.

REFERENCES

1. G. I. Kanel', S. V. Razorenov, A. V. Utkin, and V. E. Fortov, *Shock-Wave Phenomena in Condensed Media* [in Russian], Moscow, Yanus-K (1996).
2. S. A. Novikov, I. I. Divnov, and A. G. Ivanov, "Failure of steel, aluminum, and copper under explosive loading," *Fiz. Met. Metalloved.*, **25**, No. 4, 608–615 (1964).
3. G. V. Stepanov, "Spalling failure of metals loaded by plane elastoplastic waves," *Probl. Prochnosti*, No. 8, 66–70 (1976).
4. V. I. Romanchenko and G. V. Stepanov, "The effect of the time parameters of loading on the critical stresses upon spalling in copper, aluminum, and steel," *Prikl. Mekh. Tekh. Fiz.*, No. 4, 141–147 (1980).
5. V. D. Gluzman and G. I. Kanel', "Measurement of tensile stresses behind the spalling plane," *Prikl. Mekh. Tekh. Fiz.*, No. 4, 146–150 (1983).
6. A. N. Dremin and G. I. Kanel', "Compression and rarefaction waves in shock-compressed metals," *Prikl. Mekh. Tekh. Fiz.*, No. 2, 146–153 (1976).